DOI: 10.18720/MCE.89.8

Strengthening of RC beams by ferrocement made with unconventional concrete

M.J. Miah[a]*, M.S. Miah[b], W.B. Alam[c], F. Lo Monte[d], Y. Li[e]
[a] *University of Asia Pacific, Dhaka, Bangladesh*
[b] *Technische Universität Dresden — TU Dresden, Dresden, Germany*
[c] *University of Asia Pacific, Dhaka, Bangladesh*
[d] *Politecnico di Milano, Milano MI, Italy*
[e] *Nanyang Technological University, Singapore*
* E-mail: jihad.miah @uap-bd.edu

Abstract. Some countries in South Asia has very limited availability of natural stones due to geological features, therefore, most of the concrete buildings of the past are made with burnt clay brick aggregates whose strength is rather low those are more vulnerable to collapse due to any extreme loads. However, ferrocement strengthening has several advantages such as good mechanical performance, cost-effectiveness, locally availability of the materials, and simplicity, this latter making available workmanship able to implement such technique (aspect which is very important in developing countries such as Bangladesh). Hence, the paper deals with the efficacy of ferrocement technique in improving the performance of reinforced concrete beams made in low-strength concrete (beam width 230 mm, height 230 mm, and length 2135 mm). The beams are made with unconventional concrete whose strength is about 12.5–13.0 MPa. The flexural tests are performed experimentally and numerically via the finite element software ABAQUS by considering the following loading configurations: (i) 2 point loads placed at L/3, (ii) 2 point loads are to the support, (iii) 2 point loads close to the mid-span, and (iv) 1 load next to the support and 1 load on the mid-span. The experimental results have shown that unsymmetrical loading decreases the overall load carrying capacity and increases the deformability due to the localization of the damage. The ferrocement beams reinforced by steel wire mesh exhibits high ultimate load carrying capacity and more ductile behavior. The outcome of this research can be used for future modeling and for the development of appropriate design guidelines on the strengthening of concrete structures dealing with different loading conditions.

1. Introduction

Structures very often struggle with extreme static and dynamic actions during their service life, this leading to increasing damage with time, depending on the load level and on the loading layout (compression or tension, shear or bending, etc.). Hence, different caution should be considered depending on the bearing element, namely columns, beams, arches, ceilings, due to the different stress state. In the particular case of beams, the mechanical behavior is generally driven by bending, with a more or less pronounced influence of shear action, this making the load-deflection $(P-\Delta)$ relationship a powerful tool to investigate their overall performance. Within this context, an open issue is represented by unconventional concrete (i.e., very low strength concrete made with burnt clay brick aggregate), widely used in several countries in South Asia, and not properly addressed in most of the design codes, even though they cover the design details for normal concrete.

Typically, beams' behavior is critical in the case of concentrated loads, due to the high stresses induced by shear in the disturbed zone, because of the interaction among global mechanisms and local strut-and-tie systems. The cracking patterns and the damage strongly depend on the loading configurations, influencing the flexural stiffness and, consequently, the deflection characteristics. For instance, concentrated loads on

beam may locally affect the shear or moment capacity of the beam and as a result damages or sudden collapse may occur leading to catastrophic losses, this being even more evident in the case of construction materials with low quality. In many developing countries such as Bangladesh, many structures have constructed with poor construction materials and unconventional concrete. Due to the aforementioned issue, retrofitting such structures is unavoidable. Since retrofitting solutions should represent a good compromise between effectiveness and cost, this study addresses the application to low strength concrete (LSC) structures of economical (no sophisticated technology is needed) retrofitting based on the use of ferrocement.

In existing literature, just a few works including retrofitting with LSC can be found, focusing on the effect of the type of loading (related to shear and bending stress concentration). Damage pattern as a function of load configuration is reported in [1]. Several works describe the finite element analysis and also the modeling technique for considering moving loads induced by wheels and lateral load distribution in I-girders of highway bridges [2, 3]. A simplified method for evaluating load carrying capacity of structure subjected to concentrated impact load with increasing loading rate has been implemented to evaluate the load carrying capacity of RC beams with reduced effective length [4].

Results from the literature addressing the flexural characteristics of T-beams and rectangular beams retrofitted with ferrocement at the tension side showed a significant improvement of the structural performance, with a delay of the first crack formation and an increase of the overall flexural stiffness [5, 6]. By using high-performance ferrocement strengthened with U-shaped steel mesh increases the flexural capacity of beams reducing the crack formation [7]. The bending performance of retrofitted RC beams have studied by using wire mesh-epoxy composite in [8], while an experimental investigation of strengthened RC beams with FRP strips and special resins is reported in [9]. Another method for enhancing the flexural capacity is to use layers of externally bonded wire mesh by using epoxy. In addition, cracking behavior and energy absorption capacity also increases [10]. Furthermore, to reduce the weight of the retrofitting system, investigations on the use of foamed blast furnace slag to replace sand in ferrocement is also conducted [11].

In order to enhance the shear strength, the use of wire mesh in web and flange region increases the shear capacity while limiting crack opening [12]. In addition, vertical and inclined plates using glass fiber reinforced or carbon fiber reinforced polymers (GFRP or CFRP, respectively), Kevlar fiber-reinforced plastic (KFRP) and steel plate have been previously investigated in several research works, showing benefits in shear behavior [13–16]. In a recent study, the behavior of square columns with ferrocement jacket shows an improvement in ductility under cyclic and axial loading [17, 18]. RC slabs and masonry walls retrofitted with ferrocement also showed improved behavior under different types of loading [19, 20]. In a previous study [21], ferrocement retrofitting proved to be rather economical and effective to enhance the performance of partially damaged flat-plat type structures. Additionally, the ferrocement is used to enhance the shear bond performance and excellent outcome has reported in [22]. In [23] the authors studied the shear behavior of beam by performing test experimentally and numerically. Further, bending behavior of ferrocement beams with lightweight cores and different types of mesh reinforcement have been investigated and authors reported that the ferrocement can be used for low cost structures. The superior performances of ferrocement beams have reported under flexural loadings in [25]. The ferrocement jacketing with diagonal reinforcements has been used to improve the structural behavior of internal joints in [26].

In order to better understand the experimental results, numerical simulations are essential, so to generalize the specific results obtained. Numerical study on the deflection behavior of retrofitted beams with Wire Mesh-Polyurethane Cement (WM-PUC), composite and near-surface-mounted (NSM) and fiber-reinforced polymer (FRP), namely NSM-FRP rods, show a good agreement with the experimental results [27, 28]. Similarly, finite element analysis on retrofitted beams with CFRP and FRP have also been conducted to monitor $P - \varDelta$ behavior, crack pattern, and failure mode [29, 30]. Concrete with polymer composite reinforcement (FRP) instead of steel one proved the benefits of FRP when existing gap minimization between the bars is crucial [31]. The use of multilayered glass fiber to enhance the shear capacity performance of short beam is studied in [32]. The main motivation behind this research is that just a few published researches focuse on LSC. Hence, this research project has been launched to investigate the behavior of unretrofitted and retrofitted beams made with unconventional concrete (i.e., LSC).

The rest of the article is organized as follows: Section 2 describes the experimental method, including material properties, specimen detail, and test procedure. Section 3 presents the numerical investigations, including the modeling detail. Section 4 reports comparisons and discussion of the results. Finally, Section 5 includes a summary of the outcome of the study and future perspectives.

Miah M.J., Miah M.S., Alam W.B., Lo Monte F., Li Y.

2. Experimental Method

2.1. Material properties

The first class burnt clay bricks (commonly used in Bangladesh) are used as coarse aggregates, while natural river sand (locally called Sylhet sand) passing a No. 4 sieve (4.75 mm), clean and free of any deleterious substance, and of fineness modulus and specific gravity 3.1 and 2.56, respectively is used as fine aggregate. The maximum and minimum size of coarse aggregates are 20 mm and 5 mm respectively and the grading of the coarse aggregates is controlled as reported in ASTM C33 [33]. The volumetric mix ratio (commonly practiced mix design in Bangladesh) of 1:2:4 (cement: fine aggregate: coarse aggregate) and water to cement ratio (by weight) of 0.45 are used for the concrete mix. Cement CEM II/B-M is used as a binder, with 65–79 % clinker and 21–35 % mineral admixture (fly ash and slag) including gypsum. In order to evaluate concrete compressive strength, cylindrical specimens ($D \; x \; L$ = 100×200 mm) are cast and demolded after 24 hours. Afterward, all concrete specimens are cured underwater (20 ± 2 °C) up to the day of the beam specimens tests (i.e., 28 days). Compressive tests are performed at 28 days according to ASTM C39 [34] by using a Universal Testing Machine (UTM). Deformation of the specimen is measured by means of two dial gauges to investigate the stress-strain law. The average compressive strength of concrete of four batches are, respectively, 12.3, 12.8, 13.0, and 13.3 MPa (average value of 12.9 MPa with a normalized standard deviation of 3.3 %).

2.2. Preparation of Specimens

2.2.1 Preparation of Un-Retrofitted Beam Specimens

Four beams (230×230×2135 mm) are cast to evaluate the flexural performances under four different loading conditions: (i) Reference, (ii) Combined, (iii) Shear, and (iv) Bending conditions. Reference, Combined, and Shear beams are provided with 2 Ø 16 mm mild steel bars as tension reinforcements at the bottom face, while Bending beam is fitted with 3 Ø 16 mm. In the upper face (compression zone), 2 Ø 16 mm bars are used for all the beams. Shear reinforcement consists of 10 mm bars @ 127 mm c/c (center to center). The reinforcements have the yield stress of 400 MPa and elastic modulus of 200 GPa. Detailing of reinforcement arrangements are shown in Figure 1. The clear cover for the reinforcements is 40 mm for all the beams. The flexural tests are carried out after 28 days of curing.
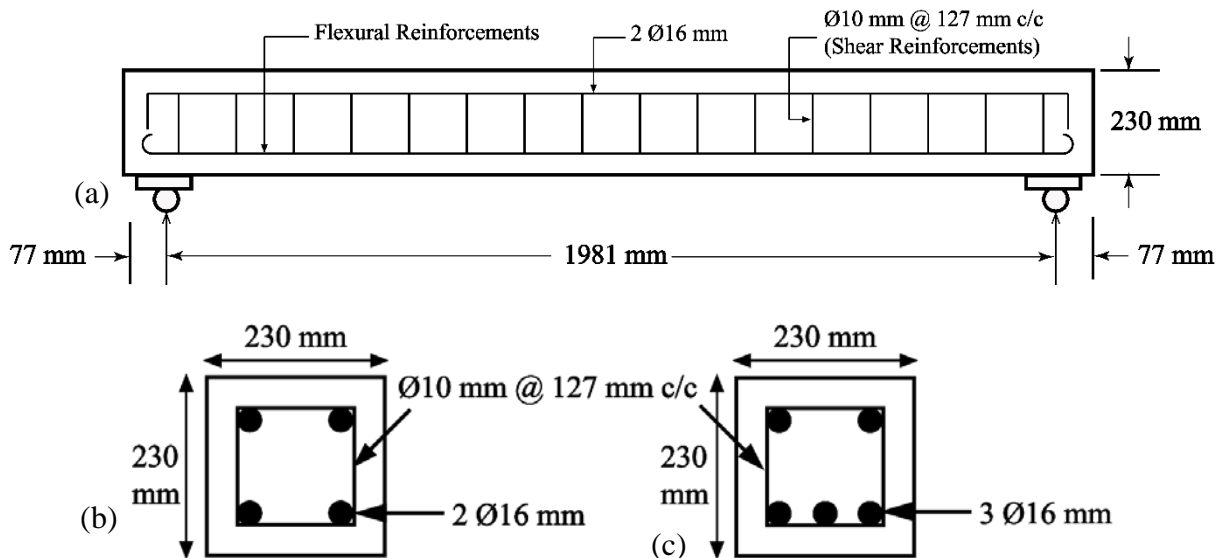

Figure 1. Reinforcement detailing of beams: (a) longitudinal view; (b) cross-section of Reference case (URRC), Combined case (URCC), and Shear case (URSC); (c) cross-section of Bending case (URBC) respectively.

2.2.2 Preparation of Retrofitted Beam Specimens

Before retrofitting, one specimen of each case is first preloaded until both flexural and diagonal major cracks appear (Figure 2a). The loads that induced the major cracks are, respectively, 82.25 kN for Reference case, 59.05 kN for Combined case, 52.42 kN for Shear case, and 62.36 kN for Bending case. Preloading is conducted via a Universal Testing Machine (UTM) with a load capacity of 1000 kN. Afterward, damaged parts are removed by using chipping hammers. Great attention needs to be paid to not damaging the reinforcing bars. The surface is then cleaned to remove the dust using a brush and a vacuum cleaner for a better bond between the original concrete surface and the retrofitting layer. For retrofitting, square welded wire steel mesh (opening of 4 mm) available in local markets is used as reinforcing mesh (Figure 2b). In order to provide confinement, the beams are wrapped with a single layer of steel wire mesh around the beam surface. The average thickness of the ferrocement mortar is about 25 mm.

Миах, М.Д., Миах М.С., Алам В.Б., Ло Монте Ф., Ли Й.

Figure 2. Retrofitting via ferrocement technique: (a) partially damaged beam, (b) the wire-mesh around the partially damaged beam, and (c) retrofitted beam before the flexural test.

The mortar for ferrocement is made with locally available ordinary Portland composite cement (CEM type II/B-M), natural river sand (Sylhet sand) with fineness modulus and specific gravity 3.1 and 2.56 respectively, and water. Sand to cement ratio by weight of 2 and water to cement ratio of 0.45 are used for the mortar mix. 25 mm thick mortar is poured around the beam specimens by hand plastering. During pouring, the mortar has forced through the steel wire mesh in order to avoid the formation of voids and to ensure good bond among mortar, wire mesh, and original concrete beam surface. Finally, the beams are covered with double layer wet burlap in the laboratory temperature of 20±2 °C in order to avoid evaporation of water from mortar and to continue hydration of cement so to guarantee better strength. After 28 days from the application of ferrocement, the beams are painted using white paint and grids are signed so that crack patterns could be easily observed during the testing process (Figure 2c). The flexural tests are performed after 28 days of curing.

2.2.3. Instrumentation and test setup

Four beams are cast to evaluate the flexural and shear performance of un-retrofitted and retrofitted beams under four different loading conditions. Beams are subjected to four-point incremental static loads with different positions of the loading points: (i) 2 point loads placed at $L/3$ interval (Reference case), (ii) 2 point loads close to the support (Shear case), (iii) 2 point loads close to the mid-span (Bending case), and (iv) 1 load next to the support and 1 load on the mid-span (Combined case). More specifically, the Reference case, designated as URRC/WRRC (un-retrofitted/retrofitted Reference Case) is subjected to a uniformly spaced concentrated loads (660 mm). For the combined effect, designated with URCC/WRCC (un-retrofitted/retrofitted Combined Case), 1 load is applied at the mid-span and the other one at 305 mm from the support, so to have high bending and shear on the loaded zone. In order to observe the behavior under shear effect (URSC/WRSC, Shear Case), loads are placed at 305 mm from the support and at 530 mm from the first load (this distance has chosen due to the limitation of test setup dimension in the lab), so generating high shear concentration. Finally, in URBC/WRBC (Bending Case), both point loads are placed across mid-span at 305 mm apart from each other. Figure 3 illustrates the loading schemes.

In order to monitor the deformation, three dial gauges with an accuracy of 10 μm are placed under the concrete beams in the steel loading frame (Figure 4). Gauge 2 is positioned at mid-span of the beam, while Gauge 1 and Gauge 3 are placed at 305 mm aside of Gauge 2. For the un-retrofitted beam tests, the beams are first loaded until major flexural and diagonal cracks appear. On the other hand, for the retrofitted beam tests, load is increased until

complete failure of the specimen. Propagation of cracks throughout the sides of the specimens are marked with black marker on the beams. Additionally, the failure patterns of the beams are also recorded.
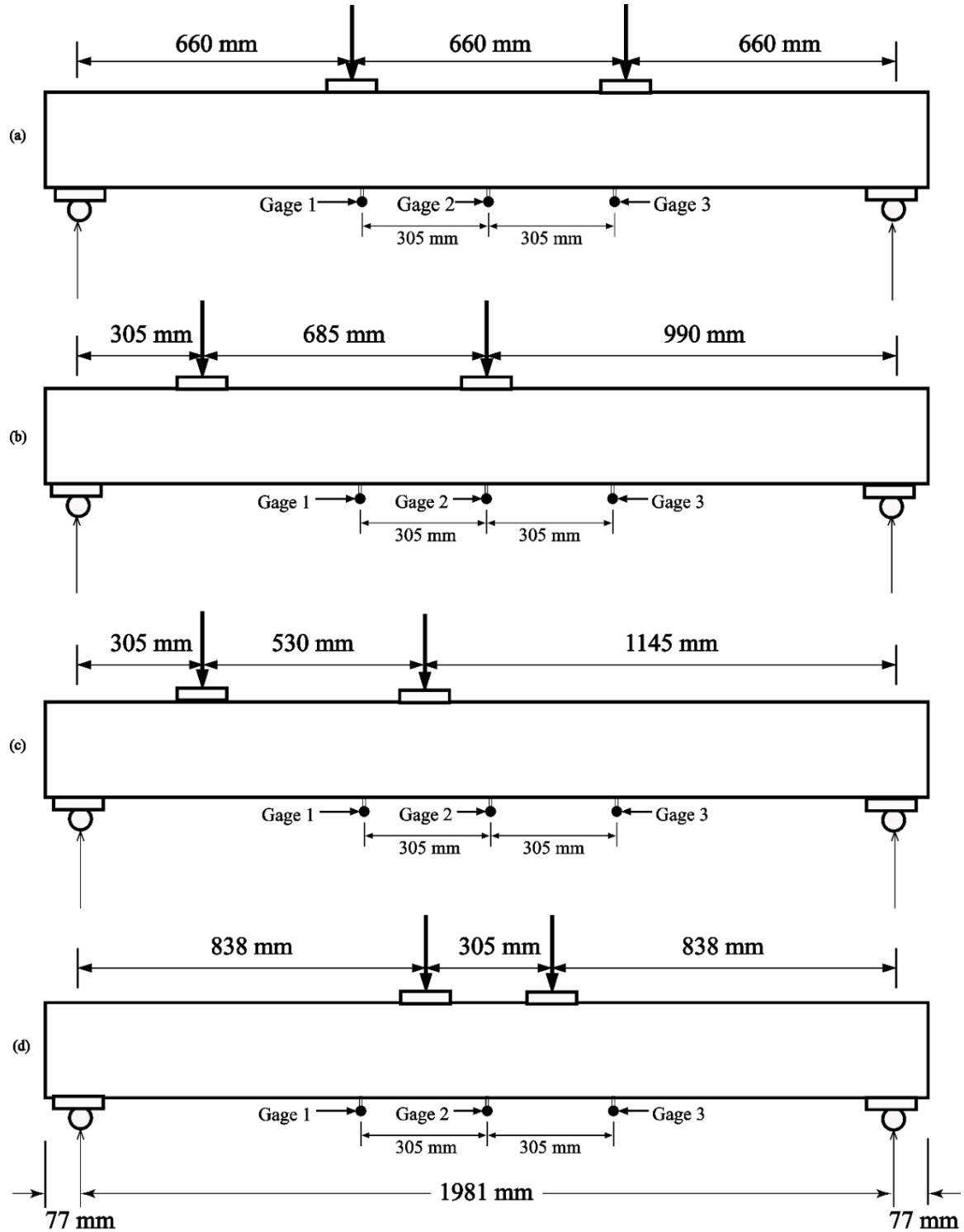

Figure 3. Schematic diagram of loading and gauge positions of the beams: (a) Reference case, (b) Combined case, (c) Shear case, and (d) Bending case respectively.

Figure 4. Beam test setup (left) and position of the dial gauges placed at steel loading frame (right).

3. Numerical Investigations

In order to better understand the experimental results, a three-dimensional nonlinear finite element model has been implemented to simulate the tests. The commercial software ABAQUS/Standard is used. All tests of un-retrofitted and retrofitted beams are presented in the followings.

3.1. Geometry and Element Types

Three-dimensional solid elements are adopted with a mesh size of 15 mm for both concrete and steel rebar depicted in Figure 5. The outer ferrocement layer is modeled as three-dimensional solid element and the wire mesh is herein embedded. Supports and loading points are modeled using a discrete rigid restraint, since the relative positions of the nodes involved remain constant throughout the simulation [35].
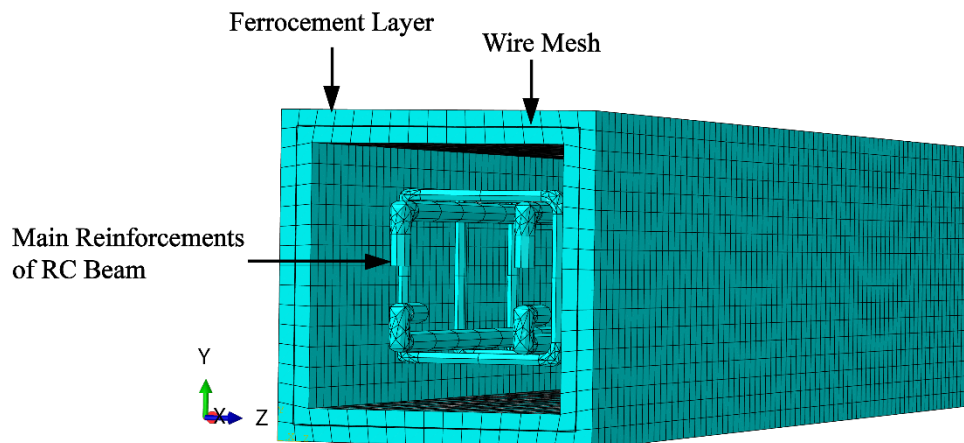

Figure 5. Numerical model in ABAQUS with the details of the retrofitted beam with embedded wire mesh inside the ferrocement layer.

3.2. Material Modeling

Concrete Damaged Plasticity model for concrete is implemented in ABAQUS and the Standard analysis is performed. The aforementioned model describes the unrecoverable stiffness reduction due to cracking processes. Concrete strength values are obtained from laboratory tests (average $f'_{c(28\,\text{days})}$ = 12.9 MPa). The behavior of the wire mesh is specified by an elastic-perfect plastic stress-strain model. For reinforcements, elastic modulus, E_s = 200 GPa and yield stress, f_y = 400 MPa are adopted. The Poisson's ratio for concrete and reinforcements are 0.2 and 0.3, respectively.

3.3. Bond between Ferrocement Layer and Concrete Surface

To define the bond between ferrocement layer and concrete surface, a tie constraint (namely perfect bond) has been implemented for the whole simulation period. The wire mesh and the main reinforcements are bonded with an embedded constraint in the host region (mortar layer and concrete, respectively). In embedded constraint, the transitional Degree Of Freedoms (DOFs) of the embedded nodes become constrained to the interpolated value of the corresponding DOFs of the host element [28]. Perfect bond between concrete and steel is adopted, since reinforcement-to-concrete bond failure has not been observed experimentally.

3.4. Boundary Condition and Solution Algorithm

Supports are placed at 77 mm from the edge of the beam. Two point loads on top of the beams are restricted to move in X (longitudinal) and Z (transverse) directions using displacement/rotation boundary conditions, and loads are applied in Y (vertical) direction.

4. Results and Discussion

In the followings, both experimental and numerical load-deflection $(P-\Delta)$ curves are shown for retrofitted and un-retrofitted beams (Reference, Combined, Shear, and Bending cases). The ultimate load carrying capacity, peak deflection, and failure pattern are also discussed herein.

4.1. Role of loading configuration on the $P-\Delta$ behavior of un-retrofitted beams

The load-deflection $(P-\Delta)$ curves at the three measuring points of un-retrofitted beams are represented in Figure 6. For the un-retrofitted beams, the loading is carried up to the formation of major cracks (e.g., flexural and diagonal). The Reference case (URRC) reached the load and deflection of 82.25 kN and 12.95 mm, respectively, which has been recorded at mid-span (gauge 2). Obviously, bending case (URBC) exhibited higher deflection than the URRC at similar load level due to the higher induced bending moment with respect to the other cases. It is also observed that the slope of the $P-\Delta$ curve is lower for the unsymmetrical loading positions (e.g., Bending case and Combined case) than the symmetrical (Reference case) ones. Despite being subjected to different loading configurations, Bending case (URBC) and Combined case (URCC) has almost similar $P-\Delta$ behavior, and their maximum deflection ranged from around 8 to 10 mm. On the other hand, for the Shear case (URSC), the final $P-\Delta$ curve is significantly lower than the other cases. This behavior could be due to the development of high concentration of shear-induced damaged close to the support (damage localization). A thick crack is observed for Shear case close to the loading point at the end of the beam, while no similar cracking or damage has been observed for the other three cases.
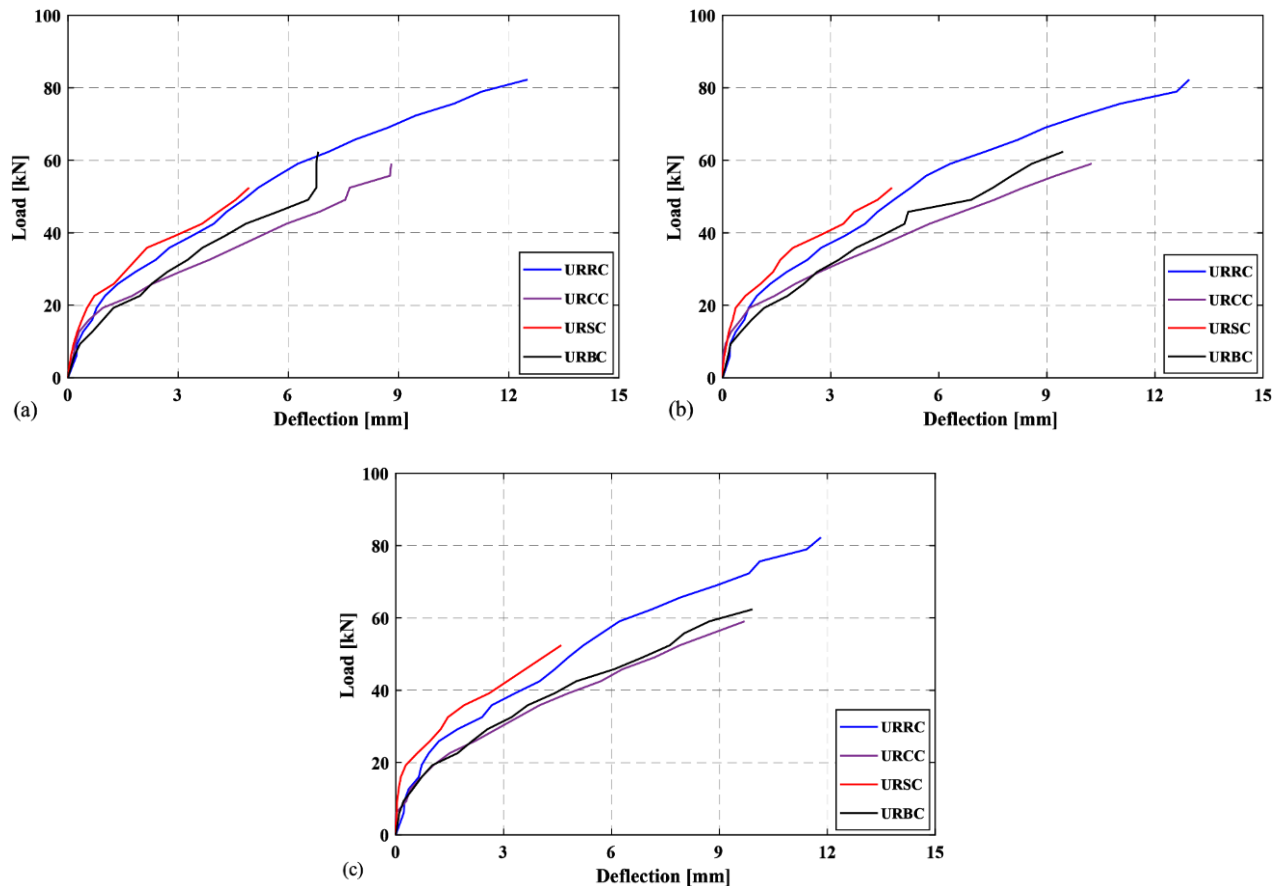

Figure 6. $P-\Delta$ **curves of un-retrofitted beams: (a) at 305 mm left from the midpoint (Gauge 1), (b) at midpoint (Gauge 2), and (c) at 305 mm right from the midpoint (Gauge 3) of the beam respectively.**

4.2. Role of ferrocement technique on the $P-\Delta$ behavior of beams

Figure 7 shows $P-\Delta$ curves for all the un-retrofitted (URRC, URCC, URSC, and URBC) and retrofitted (WRRC, WRCC, WRSC, and WRBC) beams. Except that for the Shear case, ferrocement beams exhibited an improvement, thanks to the partial prevention of crack propagation and to the additional tensile strength provided. As mentioned before, the Shear case beam was seriously damaged at the end of the first loading (before retrofitting) next to the support, thus making vain the following strengthening. In most of the cases, similar flexural behavior is observed between retrofitted and un-retrofitted beams in all the three measuring points. It is worth noting that, due to technical problems, the deflection at Gauge 3 of Combined case is not monitored.

Миах, М.Д., Миах М.С., Алам В.Б., Ло Монте Ф., Ли Й.

It should be noted that retrofitting with ferrocement allowed to mostly recover the "virgin" stiffness of the beams, as shown by the very similar trends of $P - \Delta$ curves at first loading (un-retrofitted specimens) and after damaging and retrofitting (retrofitted specimens). The overall response of the retrofitted beams demonstrated the benefit of using ferrocement technique for enhancing the flexural performance of partially damaged structures, for example, due to earthquake, wind load, blast and fire. This is in agreement with the results of previous tests on flat plate systems reported in [36]. Similar behavior is observed in the literature [5–7, 24]. It is also observed that the first crack is delayed in retrofitted beams with respect to the un-retrofitted beams.
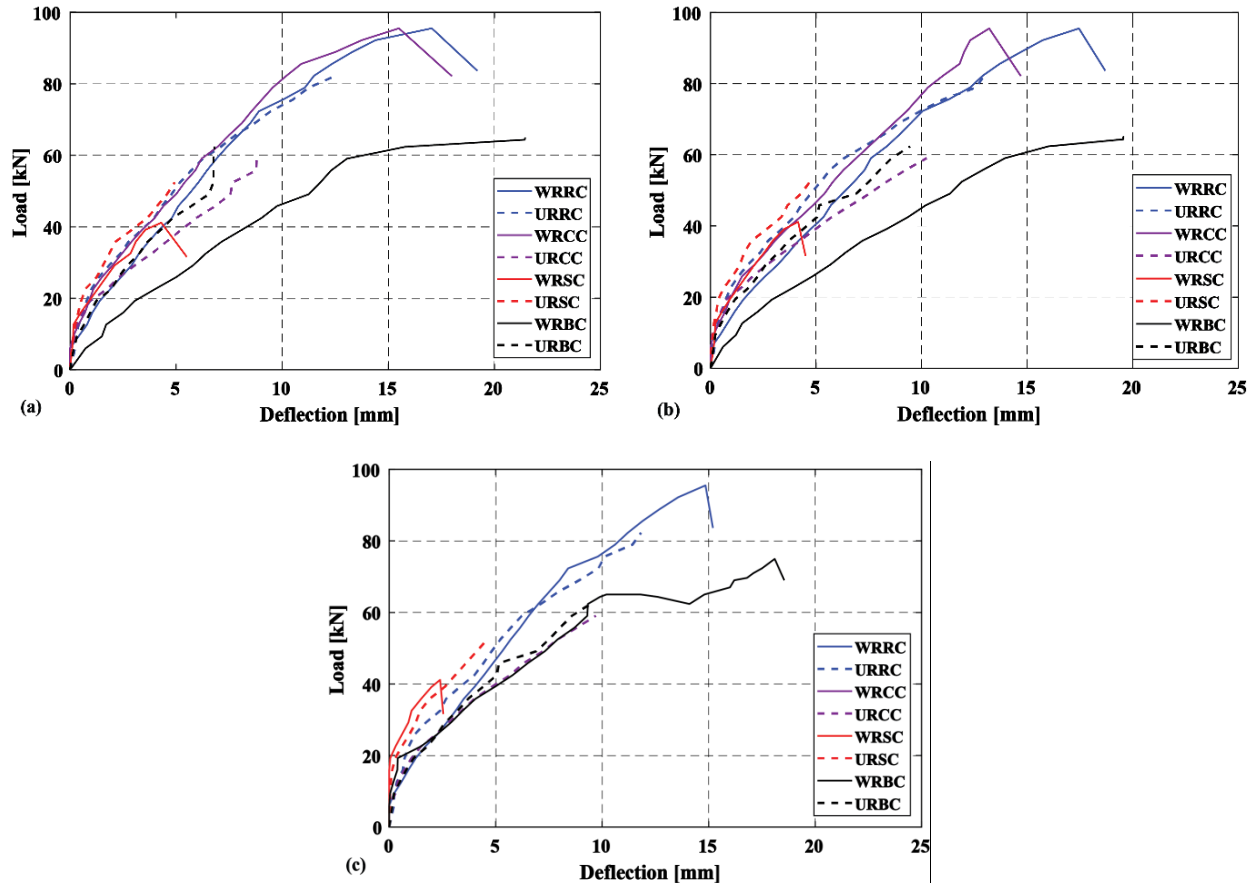

Figure 7. Comparison of $P - \Delta$ **behavior of un-retrofitted and retrofitted beams: (a) at 305 mm left from the midpoint (Gauge 1), (b) at midpoint (Gauge 2), and (c) at 305 mm right from the midpoint (Gauge 3) of the beams correspondingly.**

It can be noticed that the retrofitted Reference (WRRC) and Combined (WRCC) cases collapsed at almost the same load, despite the different loading configuration. However, the deflection of Combined case is significantly lower than the Reference case due to higher shear stress. Among all the cases, except Shear case (since it collapses earlier due to pre-damage of the beam), the Bending case showed the lowest load-bearing capacity due to the significantly higher bending moment with respect to the other three cases. However, ductility is significantly improved in most of the ferrocement beams. In general, it is observed that retrofitting with steel wire mesh combined with ferrocement improves the flexural behavior and load carrying capacity for the different loading configurations, by limiting the formation of cracks and micro-cracks. Thanks to the strengthening process, the wire mesh embedded in ferrocement provided an effective further contribution in tension, allowing an increase of the load-bearing capacity. A further benefit probably is the lateral confinement provided by the retrofitting, so limiting the propagation of cracks and improving the shear behavior close to the supports. Both Reference case and Combined case of retrofitted beams reached the maximum load of 95.5 kN and the retrofitted Bending case attained 75.0 kN.

4.3. Failure pattern of the retrofitted beams

The cracking patterns of the retrofitted beams at failure is presented in Figure 8. The figure indicates that there is a significant difference in failure patterns depending on the loading configuration. In Reference and Combined cases, a marked distribution of cracks are observed all along the length showing a combination of bending and shear collapse, while in Shear and Bending cases the damage is concentrated at the support or in the mid-span, respectively, due to shear or bending-induced collapse. Ductile mode of failure is observed for Reference and Bending cases thanks to multiple cracking, while a brittle failure has seen for the Shear

case. As regards the retrofitting system, yielding of the steel wire mesh probably occurred before debonding between the steel wire mesh and original concrete surface, and then finally the retrofitted beam failed with significant higher deflection.

The numerical $P - \Delta$ behavior of un-retrofitted beams is compared with the experimental results and presented in Figure 9 (a–d). The figure shows a rather good agreement between measured and predicted deflections for the four un-retrofitted beams, with just a slight underestimation of the initial stiffness.
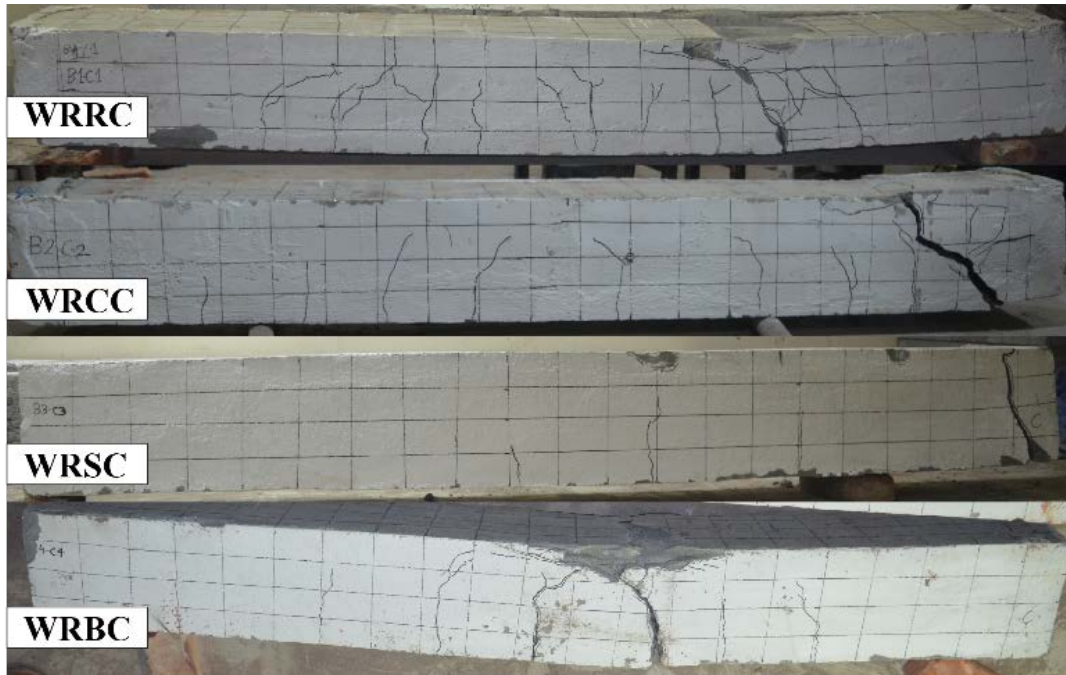

Figure 8. Crack pattern of the retrofitted beams tested in four different loading positions.

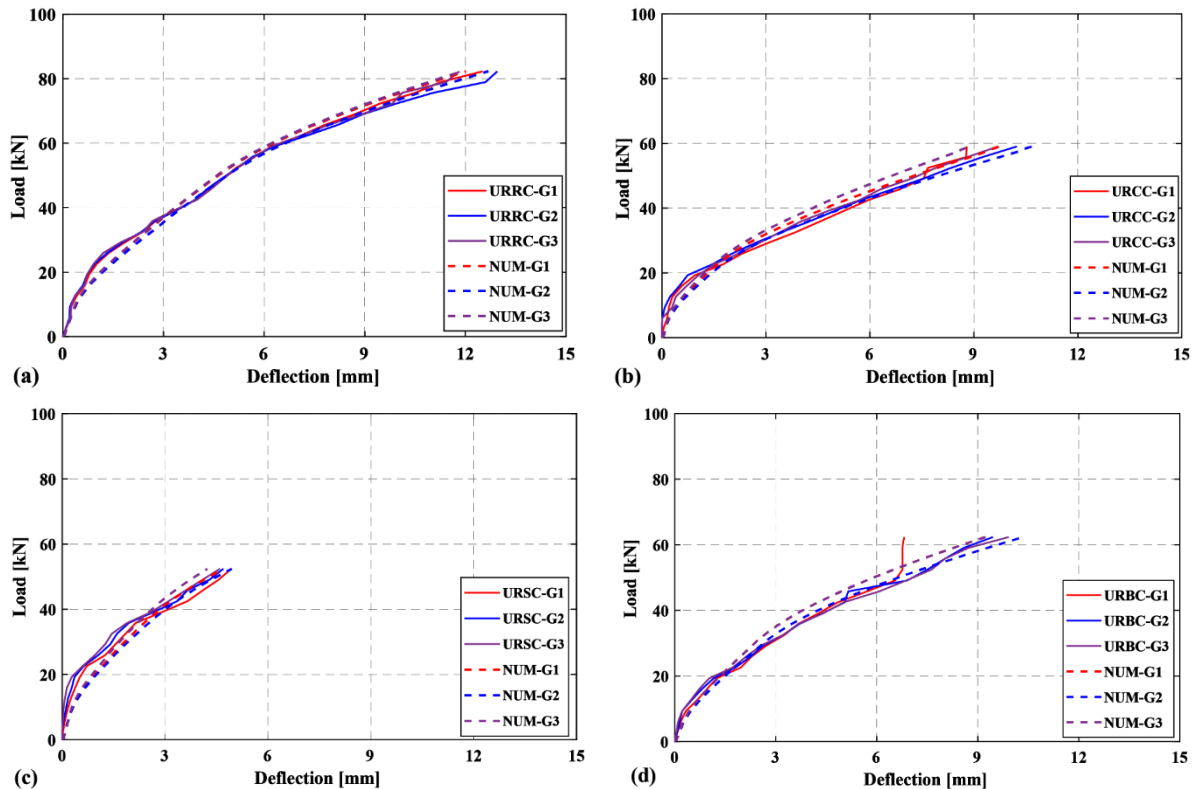### 4.4. Numerical $P - \Delta$ behavior

Figure 9. Comparison of experimental and numerical $P - \Delta$ curves of un-retrofitted beams: (a) Reference case, (b) Combined case, (c) Shear case, and (d) Bending case respectively.

As concern the retrofitted beams, the numerical deflections calculated at three different positions are quite similar to the experimental results, especially for the Combined case (see Figure 10). The differences can be

Миах, М.Д., Миах М.С., Алам В.Б., Ло Монте Ф., Ли Й.

ascribed to the fact that the partial damage of the beams before applying ferrocement is not taken into account in the numerical model. Probably, because of that reason, the numerical slope of the load-deflection curve is higher than the experimental curves. Furthermore, the ferrocement behavior is a bit more complicated than the RC beam due to different role of different materials such as steel wire mesh, reinforced concrete and cement mortar, in addition to steel-concrete bond stiffness. Finally, the plots of plastic strain distribution in the retrofitted beams are shown in Figure 11. As expected, except Shear case, the higher stain occurred near the mid-span (i.e., gauge G2) of the beam as observed in Figure 11. The rather good agreement between numerical and experimental results corroborate the idea that no significant debonding occurred at the ferrocement to beam interface.
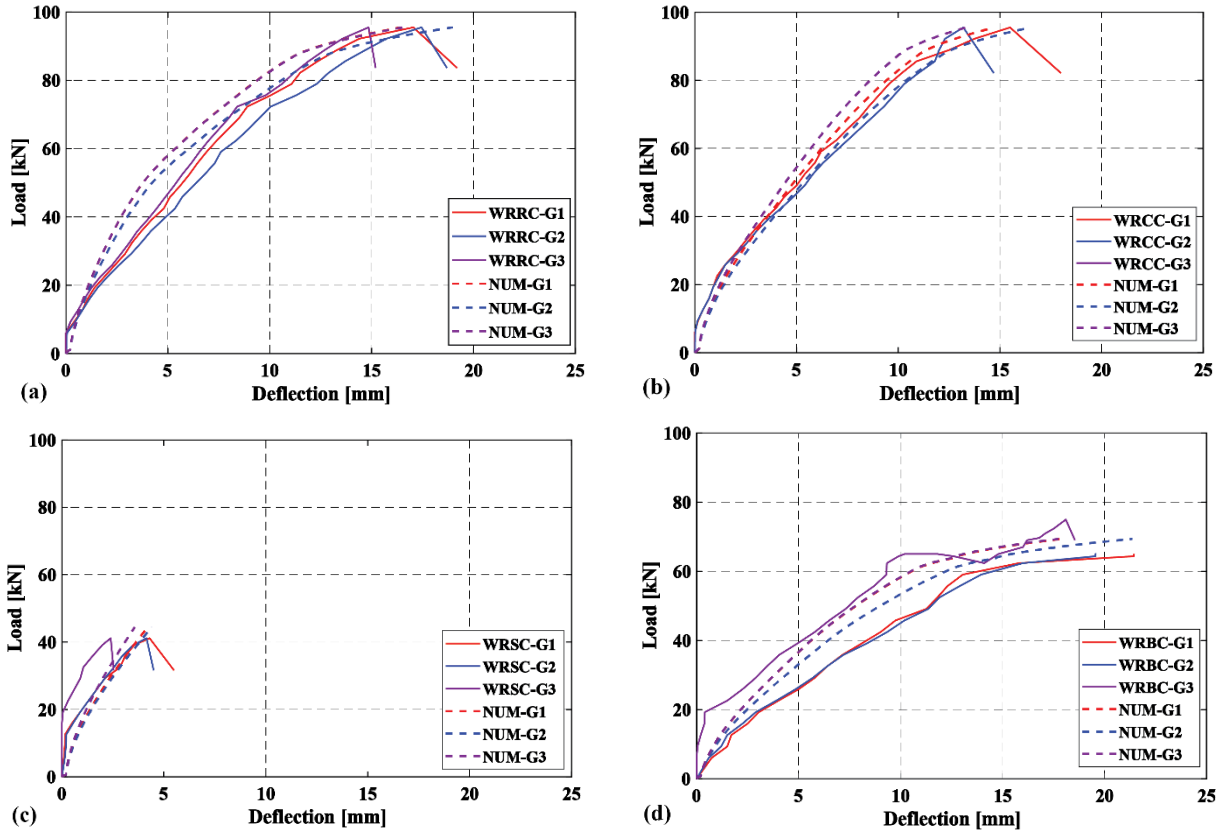

Figure 10. Comparison of experimental and numerical $P - \Delta$ curves of beams:
(a) Reference case, (b) Combined case, (c) Shear case, and (d) Bending case correspondingly.
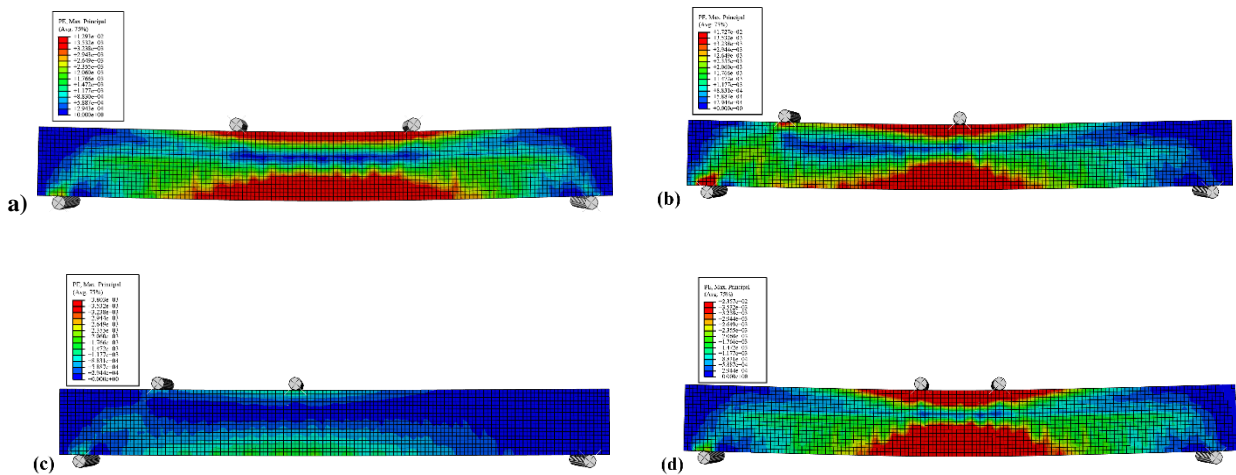

Figure 11. 3D image of plastic strain distribution in the retrofitted beams at the end of loading:
(a) Reference case, (b) Combined case, (c) Shear case, and (d) Bending case respectively.

5. Conclusions

This study is carried out on RC un-retrofitted and retrofitted beams made with unconventional concrete (i.e., very low strength concrete – LSC at 28 days ≈ 12.5–13.0 MPa) under four-point incremental static loading. In order to gain a deeper understanding of the role of loading positions on the flexural performance of the beams, numerical simulations have been performed via the finite element software ABAQUS. Four-point

flexural tests are performed experimentally and numerically on both retrofitted and un-retrofitted beams with different loading positions: (i) 2 loads at $L/3$ (Reference case), (ii) 2 loads close to the support (Shear case), (iii) 2 loads close to the mid-span (Bending case), and (iv) 1 load next to the support and 1 load on the mid-span (Combined case). The following conclusions can be drawn based on the results presented in this research work:

– The beams tested under unsymmetrical loading show a worse mechanical performance due to shear action. Among four cases, poor performance of RC beam is observed in Shear case which is associated to the formation of major crack at the end of the beam (shear failure).

– Ductile mode of failure is observed for the Reference and Bending cases in retrofitted beams, while a brittle failure has seen for the Shear case due to severe cracking with damage localization occurred during the pre-cracking phase on the un-retrofitted beam.

– Numerical results of un-retrofitted and retrofitted tests are in quite good agreement with the experimental results. In numerical analyses retrofitting debonding is not considered, this corroborating the idea that ferrocement-to-beam bond has been effective.

– Ferrocement technique is cheap, sustainability, achievable with local materials and ordinary (namely, not specialized) workmanship, light in weight (i.e., lower self-weight, so reducing the increase of the permanent load on the structure to be retrofitted), and efficient in construction time. Therefore, it could be recommended to use ferrocement technique to strengthen existing structures made with low strength concrete to avoid sudden collapse due to extreme loading, such as earthquake.

Though a better performance of ferrocement retrofitted beams have been observed, it is essential to study other important issues, such as the bond between ferrocement and original concrete (i.e., ferrocement jacketing), the possible benefits in ductility brought in by adding different layer of wire mesh or by the introduction of steel or natural fibers in the mortar, the durability performance of ferrocement due to its lower net cover and the higher surface area of the reinforcement (i.e., higher risk of corrosion), the lower density of the mortar (i.e., higher penetration of water, higher corrosion) as well as dynamic and fire behavior. This is an ongoing research project where further work is planned in the direction of strengthening of beam-column structures made with low strength concrete subjected to gravitational loads or to extreme events such as earthquake or fire.

6. Acknowledgements

References

1. Raoof, M., Lin, Z. Structural characteristics of RC beams with exposed main steel. In Proceedings of the Institution of Civil Engineers – Structures and Building. 1997. 122(1). Pp. 35–51.

2. Tarhini, K.M., Frederick, G.R. Wheel load distribution in I-girder highway bridges. Journal of Structural Engineering. 1992. 118(5). Pp. 1285–1294.

3. Tarhini, K.M., Frederick, G.R. Lateral load distribution in I-girder bridges. Computers & structures. 1995. 54(2). Pp. 351–354.

4. Cotsovos, D.M. A simplified approach for assessing the load-carrying capacity of reinforced concrete beams under concentrated load applied at high rates. International Journal of Impact Engineering. 2010. 37(8). Pp. 907–917.

5. Paramasivam, P.K., Ong, C.G., Lim, C.T.E. Ferrocement Laminates for Strengthening RC T-Beams. Cement & Concrete Composites. 1994. Vol. 16. Pp. 143–152.

6. Paramasivam, P., Lim, C.T.E., Ong, C.G. Strengthening of RC Beams with Ferrocement Laminates. Cement and Concrete Composites. 1998. Vol. 20. Pp. 53–65.

7. Liao, H.P., Fang, S.S. An experimental study on flexural behavior of reinforced concrete beams strengthened with high-performance ferrocement. Advanced Materials Research. 2011. Vol. 163. Pp. 3772–3776.

8. Qeshta, I.M., Shafigh, P., Jumaat, M.Z. Flexural behaviour of RC beams strengthened with wire mesh-epoxy composite. Construction and Building Materials. 2015. Vol. 79. Pp. 104–114.

9. Gao, B., Kim, J.K., Leung, C.K. Experimental study on RC beams with FRP strips bonded with rubber modified resins. Composites Science and Technology. 2004. 64(16). Pp. 2557–2564.

10. Qeshta, I.M., Shafigh, P., Jumaat, M.Z., Abdulla, A.I., Ibrahim, Z., Alengaram, U.J. The use of wire mesh–epoxy composite for enhancing the flexural performance of concrete beams. Materials & Design. 2014. Vol. 60. Pp. 250–259.

11. Desayi, P., Reddy, V. Strength of ligthweight ferrocement in flexure. Cement and Concrete Composites. 1991. 13(1). Pp. 13–20.

12. Al-Sulaimani, G.J., Basunbul, I.A., Mousselhy, E.A. Shear behavior of ferrocement box beams. Cement and Concrete Composites. 1991. 13(1). Pp. 29–36.

13. Sundarraja, M.C., Rajamohan, S. Strengthening of RC beams in shear using GFRP inclined strips–An experimental study. Construction and building materials. 2009. 23(2). Pp. 856–864.

14. Obaidat, Y.T., Heyden, S., Dahlblom, O., Abu-Farsakh, G., Abdel-Jawad, Y. Retrofitting of reinforced concrete beams using composite laminates. Construction and Building Materials. 2011. 25(2). Pp. 591–597.

Миах, М.Д., Миах М.С., Алам В.Б., Ло Монте Ф., Ли Й.

15. Alam, M.A., Hassan, A., Muda, Z.C. Development of kenaf fibre reinforced polymer laminate for shear strengthening of reinforced concrete beam. Materials and Structures. 2016. 49(3). Pp. 795–811.

16. Alam, M.A., Jabbar, A.S.A., Jumaat, M.Z., Mustapha, K.N. Effective Method of Repairing RC Beam Using Externally Bonded Steel Plate. Applied Mechanics and Materials. 2014. Vol. 567. Pp. 399–404.

17. Takiguchi, K. An investigation into the behavior and strength of reinforced concrete columns strengthened with ferrocement jackets. Cement and Concrete Composites. 2003. 25(2). Pp. 233–242.

18. Kaish, A.B.M.A., Alam, M.R., Jamil, M., Zain, M.F.M, Wahed, M.A. Improved ferrocement jacketing for restrengthening of square RC short column. Construction and Building Materials. 2012. Vol. 36. Pp. 228–237.

19. Hago, A.W., Al-Jabri, K.S., Alnuaimi, A.S., Al-Moqbali, H., Al-Kubaisy, M.A. Ultimate and service behavior of ferrocement roof slab panels. Construction and Building Materials. 2005. 19(1). Pp. 31–37.

20. Ashraf, M., Khan, A.N., Naseer, A., Ali, Q., Alam, B. Seismic behavior of unreinforced and confined brick masonry walls before and after ferrocement overlay retrofitting. International Journal of Architectural Heritage. 2012. 6(6). Pp. 665–688.

21. Miah, M.S., Miah, M.J., Hossain, M.M., Paul, S.C. Seismic Retrofit of Flat Plate and Flat Slabs Using Ferrocement, Proceedings of 5th International Congress on Technology Engineering and Science, Kuala Lumpur, Malaysia. 2018. Pp. 317–326.

22. Li, B., Lam, E.S.S. Influence of interfacial characteristics on the shear bond behaviour between concrete and ferrocement. Construction and Building Materials. 2018. Vol. 176. Pp. 462–469.

23. El-Sayed, T.A., Erfan, A.M. Improving shear strength of beams using ferrocement composite. Construction and Building Materials. 2018. Vol. 172. Pp. 608–617.

24. Shaaban, I.G., Shaheen, Y.B., Elsayed, E.L., Kamal, O.A., Adesina, P.A. Flexural characteristics of lightweight ferrocement beams with various types of core materials and mesh reinforcement. Construction and Building Materials. 2018. Vol. 171. Pp. 802–816.

25. Shaaban, I.G., Shaheen, Y.B.I., Elsayed, E.L., Kamal, O.A., Adesina, P.A. Flexural behaviour and theoretical prediction of lightweight ferrocement composite beams. Case Studies in Construction Materials. 2018. Vol. 9. e00204.

26. Li, B., Lam, E.S.S., Wu, B., Wang, Y.Y. Experimental investigation on reinforced concrete interior beam–column joints rehabilitated by ferrocement jackets. Engineering Structures. 2013. Vol. 56. Pp. 897–909.

27. Zhang, K., Sun, Q. The use of Wire Mesh-Polyurethane Cement (WM-PUC) composite to strengthen RC T-beams under flexure. Journal of Building Engineering. 2018. Vol. 15. Pp. 122–136.

28. Hawileh, R.A. Nonlinear finite element modeling of RC beams strengthened with NSM FRP rods. Construction and Building Materials. 2012. 27(1). Pp. 461–471.

29. Obaidat, Y.T., Heyden, S., Dahlblom, O. The effect of CFRP and CFRP/concrete interface models when modelling retrofitted RC beams with FEM. Composite Structures. 2010. 92(6). Pp. 1391–1398.

30. Kishi, N., Zhang, G., Mikami, H. Numerical cracking and debonding analysis of RC beams reinforced with FRP sheet. Journal of Composites for Construction. 2005. 9(6). Pp. 507–514.

31. Gizdatullin, G.A., Khusainov, R.R., Khozin, V.G., Krasinikova, N.M. Strength and deformability of concrete structures reinforced with fibre-reinforced polymer bars. Magazine of Civil Engineering. 2016. 62(2). Pp. 32–41. DOI:10.5862/MCE.62.4

32. Boldyreva, A.A., Yarunicheva, Y.A., Dernakova, A.V., Ivashov, I.I. The strength of the polymer composite (fiberglass) with interlaminar shear. Magazine of Civil Engineering. 2016. Vol. 62. No. 2. Pp. 42–50. DOI: 10.5862/MCE.62.5

33. ASTM C33, Standard Specification for Concrete Aggregates. ASTM International, West Conshohocken, PA, USA, 2003. 11 p.

34. ASTM C39, Standard Test Method for Compressive Strength of Cylindrical Concrete Specimens. ASTM Standard, West Conshohocken, PA, USA, 2005. 16 p.

35. ABAQUS. ABAQUS/standard version 6.10 user's manuals: volumes I-III, Hibbitt, Karlsson, and Sorenson, Inc., Pawtucket (RI), 2010.

36. Miah, M.S., Miah, M.J., Hossain, M.M., Paul, S.C. Nonlinear Seismic Response of Flat Plate Systems made with Ultra Low Strength Concrete. Global Science and Technology Journal. 2018. 6(2). Pp. 35–46.

Contacts:

Md Jihad Miah, +880258157091; jihad.miah@uap-bd.edu

Mohammad Shamim Miah, +4917632415430; mohammad_shamim.miah@tu-dresden.de

Walid Bin Alam, +8801682077158; walidbin.alam40@gmail.com

Francesco Lo Monte, +393331845409; francesco.lo@polimi.it

Ye Li, +6583586646; LIYE0006@e.ntu.edu.sg